

Genome-wide expanding of genetic evolution and potential pathogenicity in *Vibrio alginolyticus*

Zhenzhou Huang^{a,b,*}, Yanjun Li^{c,*}, Keyi Yu^a, Lizhi Ma^d, Bo Pang^a, Qin Qin^a, Jie Li^a, Duochun Wang^a, He Gao^a and Biao Kan^a

^aNational Key Laboratory of Intelligent Tracking and Forecasting for Infectious Diseases, National Institute for Communicable Disease Control and Prevention, Chinese Center for Disease Control and Prevention, Beijing, People's Republic of China; ^bHangzhou Center for Disease Control and Prevention, Zhejiang, People's Republic of China; ^cThe Sixth Medical Center of PLA General Hospital, Beijing, People's Republic of China; ^dThe Third Medical Center, Chinese PLA (People's Liberation Army) General Hospital, Beijing, People's Republic of China

ABSTRACT

Vibrio alginolyticus, an emergent species of *Vibrio* genus, exists in aquatic and marine environments. It has undergone genetic diversification, but its detailed genomic diversity is still unclear. Here, we performed a multi-dimensional comparative genomic analysis to explore the population phylogeny, virulence-related genes and potential drug resistance genes of 184 *V. alginolyticus* isolates. Although genetic diversity is complex, we analysed the population structure using three sub-datasets, including the subdivision for three lineages into sublineages and the distribution of strains in the marine ecological niche. Accessory genes, most of which reclassified *V. alginolyticus* genomes as different but with relatively close affinities, were nonuniformly distributed among these isolates. We demonstrated that the spread of some post-evolutionary isolates (mainly L3 strains isolated from Chinese territorial seas) was likely to be closely related to human activities, whereas other more ancestral strains (strains in the L1 and L2) tended to be locally endemic and formed clonal complex groups. In terms of pathogenicity, the potential virulence factors were mainly associated with toxin, adherence, motility, chemotaxis, and the type III secretion system (T3SS). We also found five types of antibacterial drug resistance genes. The prevalence of β -lactam resistance genes was 100%, which indicated that there may be a potential risk of natural resistance to β -lactam drugs. Our study reveals insights into genomic characteristics, evolution and potential virulence-associated gene profiles of *V. alginolyticus*.





ARTICLE HISTORY Received 18 January 2024; Revised 24 April 2024; Accepted 26 April 2024

KEYWORDS *Vibrio alginolyticus*; whole genome sequencing; population structure; virulence-related factors; antibiotic resistance genes


Introduction

Vibrio alginolyticus, a halophilic bacterium in the genus of *Vibrio*, is widely distributed in marine and estuarine habitats such as seawaters, estuaries, ocean sediment, and aquaculture settings [1]. *V. alginolyticus* was previously listed as a biotype of *V. parahaemolyticus* in the 8th edition of *Bergey's Manual of Systematic Bacteriology*, and became a separate species in the 9th edition of the manual [2]. *V. alginolyticus* is an emerging opportunistic pathogen to humans that causes foodborne diarrhoea in coastal areas [3]. Additionally, it can cause otitis media [4], soft tissue infections [5], conjunctivitis, and sepsis [3,6,7]. This bacterium also has pathogenic effects on marine organisms, including farm fish, molluscs, shellfish, and shrimp [8], and represents a sustained threat to aquaculture industries and ecosystems around the world [9].

Climate change and marine traffic lead to changing *Vibrio* species communities in the oceans [10]. As a mesophilic bacterium, pathogenic *V. alginolyticus* could become significant even in temperate zones such as the coastal areas of northern China and Europe. In our recent investigation, the increasing incidence of *V. alginolyticus* infection was found to threaten human health in coastal areas in China [11,12]. The major virulence factors of *V. alginolyticus* are motility, biofilm, extracellular proteases, type III secretion systems (T3SS), and type VI secretion systems (T6SS) [13–15]. *V. alginolyticus* shares relatively high similarities with closely related species in the Parahaemolyticus clade of the genus *Vibrio* [16]. *V. alginolyticus* and *V. parahaemolyticus* have similar genotypes [17], niche adaptations [18], and biomedical applications [19]. Flagellar motility plays an important role in the lifestyle of

CONTACT He Gao  gaohe@icdc.cn  National Key Laboratory of Intelligent Tracking and Forecasting for Infectious Diseases, National Institute for Communicable Disease Control and Prevention, Chinese Center for Disease Control and Prevention, Beijing 102206, People's Republic of China; Biao Kan  kanbiao@icdc.cn  National Key Laboratory of Intelligent Tracking and Forecasting for Infectious Diseases, National Institute for Communicable Disease Control and Prevention, Chinese Center for Disease Control and Prevention, Changbai Road 155, Changping, Beijing, 102206, People's Republic of China

*These authors contributed equally to this work.

 Supplemental data for this article can be accessed online at <https://doi.org/10.1080/22221751.2024.2350164>.

© 2024 National Institute for Communicable Disease Control and Prevention, Chinese Center for Disease Control and Prevention. This is an Open Access article distributed under the terms of the Creative Commons Attribution-NonCommercial License (<http://creativecommons.org/licenses/by-nc/4.0/>), which permits unrestricted non-commercial use, distribution, and reproduction in any medium, provided the original work is properly cited. The terms on which this article has been published allow the posting of the Accepted Manuscript in a repository by the author(s) or with their consent.

V. alginolyticus, both in the aquatic environment and in host colonization [20], and is associated with movement, colonization, adhesion, biofilm formation, and virulence. The regulation of adhesion in *V. alginolyticus* can be attributed in several chemotactic factors (such as the genes *mcp*, *cheB*, and *cheV*) [21,22].

To gain a comprehensive understanding of the genetic mechanisms shaping the epidemic dynamics of *V. alginolyticus* in the marine environment, we performed multi-dimensional comparative genomics research in this study. The rapid development of high-throughput sequencing technology in recent years has allowed the accumulation of genome data, which has provided opportunities for the genomics research on these pathogenic bacteria. Genome sequences of some *V. alginolyticus* strains have been reported in recent years [23,24], but the genomic characters were only presented for a single strain. To date, genomic variation characteristics related to horizontal gene transfer (HGT) through mobile genetic elements (MGEs) of *V. alginolyticus* has been described [25]. However, there is still a lack of genome studies related to the evolution and clonal structure of the *V. alginolyticus* population. Additionally, the phylogenetic relationships among *V. alginolyticus* strains isolated from marine environment and patients remain unclear. Little is known about the abundance, pathogenicity, and ecology of *V. alginolyticus*.

In this study, 184 strains from different regions and different host origins were genetically investigated to obtain the core- and pan-genome features, virulence-related genes, drug resistance genes, and transmission characteristics of *V. alginolyticus*. Here, we not only revealed unprecedented details of the population structure in *V. alginolyticus*, but also provided an overall analysis of virulence-related factors.

Materials and methods

Sampling, isolation and DNA extraction

Free-living, plankton-attached and shellfish-associated *V. alginolyticus* were collected between May 2008 and January 2020 in China. A total of 133 *V. alginolyticus* strains were isolated from seawater, seafood, freshwater, and other samples. Strains were cultured on 1% NaCl lysogeny broth (LB, w/v) agar at 35°C for 18 h. All strains collected in this study are listed in Supplementary Table S1.

Genomic DNA with no contamination or DNA degradation was prepared by using the QIAamp DNA Mini Kit (Qiagen, Dusseldorf, Germany). Then, a NanoDrop spectrophotometer was used to measure the concentration and purity of DNA genomes. Subsequently, the DNA integrity was checked by agarose gel electrophoresis. The quality

requirements were concentration ≥ 100 ng/ μ L and total amount > 20 μ g.

Whole genome sequencing

The genomes of 133 *V. alginolyticus* strains were sequenced using the Illumina HiSeq 4000 platform (Illumina Inc., San Diego, CA, USA) at the Beijing Genomics Institute (BGI, Shenzhen, China) with a depth of 200 \times coverage. Library construction (paired-end read sizes of 150 bp), genome sequencing, and data pipelining were performed in accordance with the manufacturer's protocols.

Genome assembly and annotation

FastQC (<http://www.bioinformatics.babraham.ac.uk/projects/fastqc/>) was applied to evaluate the raw sequence data, and the low-quality reads were filtered. The data filtering criteria were removal of contaminated adapters, removal of repeated reads, and removal of low-quality reads (Phred score ≤ 20 bases exceeding 50% of the read length). Then, the clean data were assembled into contigs using SPAdes v3.8.2 with the default parameters [26]. After removing contigs with lengths < 500 bp, QUAST v5.0.1 was applied to evaluate the genome assembly [27]. Open reading frame prediction and annotation were performed by Prodigal v2.6.3 [28] and Prokka v1.13.3 [29].

V. alginolyticus genomes from NCBI

In addition to 133 laboratory isolates, there were 61 whole genomic sequences available at the NCBI GenBank database (<https://www.ncbi.nlm.nih.gov/>) as of March 2021. Because of the existence of mislabelled species, species-level identification was clarified by average nucleotide identity (ANI) analysis. High-quality sequenced genomes were screened by using the criteria of 4.5 Mb \leq genome size \leq 6.5 Mb and contigs < 200 . A total of 51 strains from online databases were screened out and listed in Supplementary Table S2.

Average nucleotide identity (ANI) analysis

A Perl script based on the previous algorithm [30] was used to compute the ANIs for the draft sequences from the *V. alginolyticus* strains. The ANI was evaluated between the query genome and the reference genome, and the mean identity of all BLASTn matches was computed as the ANI value. The computation required that the BLASTn matches should have $\geq 30\%$ sequence identity and $\geq 70\%$ length coverage.

Pan-genome analysis

After obtaining the annotated assemblies in GFF3 format (produced by Prokka software), the pan genome matrix of *V. alginolyticus* was calculated using Roary v1.12 [31] (<https://sanger-pathogens.github.io/Roary>), a pan genome pipeline, with the identity parameter set to 90%. The heatmap of the presence/absence of pan genes was drawn in R with the gplots 3.1.1 package.

Phylogenetic tree construction

Coding sequences (CDSs) were predicted using Prodigal v2.6.3 in the *V. alginolyticus* genome sequences. A non-redundant homologous gene set was done by CD-hit v4.6.6 [32]. Then BLAST+ was applied to search for the homologous genes of the CDS of each strain in the non-redundant homologous gene set. Each homologous gene contained in all strains with a single copy was considered a core gene. Next, core SNPs were called using snippy v4.3.6 (<https://github.com/tseemann/snippy>) from all the predicted core genes against the reference genome sequence of strain ATCC 17749^T (BioSample accession: SAMN02603463). Gubbins v2.4.1 was used as a recombination-removal tool to analyse the clonal recombination relationships [33]. The fastBAPS algorithm (<https://github.com/gtonkinhill/fastbaps/>) was used to rapidly identify genomic lineages or genetic clusters [34]. The maximum-likelihood tree was reconstructed using PhyML v3.1 based on core SNPs with 1000 bootstraps.

Virulence-related gene searching

The Virulence Factor Database (VFDB, <http://www.mgc.ac.cn/VFs/>) was used to predict and annotate the virulence genes. All the protein sequences from the *V. alginolyticus* strains were searched against the VFDB using BLASTp with an E-value of 1e-5. The virulence genes were determined by using a relatively relaxed cutoff (identity \geq 80%, length coverage \geq 50%) and a stricter cutoff (identity \geq 90%, length coverage \geq 80%). Sequence alignment analysis and phylogenetic construction of a neighbor-joining (NJ) tree were performed with 1000 bootstrap replicates.

Antibiotic resistance gene searching

The antibiotic resistance genes were detected using the ResFinder tool (<https://cge.cbs.dtu.dk/services/ResFinder/>) and were cross-compared with the Comprehensive Antibiotic Resistance Database (CARD, <http://arpcard.mcmaster.ca>). The BLASTn cutoff

values were chosen as follows: E-value of 1e-5, identity \geq 90%, and length coverage \geq 60%.

Type III secretion system (T3SS) identification

The CDSs of T3SS from *V. alginolyticus* strain E06333 (Accession No.: CP071058.1) were used as references for comparison with genomes using BLAST+. For a single CDS, the alignments of more than half the length and identity $>$ 50% were considered positive matches, and the e-value cutoff was set to a lower cutoff, 1e-2. A concatenated segment of more than three regions positively mapped to the reference CDS was considered a potential T3SS segment. This screening process was conducted by an automatic pipeline.

In vitro cytotoxicity assays

Bacterial infection was performed using the human epidermoid carcinoma cell line Hep-2 (CCC0068; Peking Union Medical College Cell Resource Center). Cytotoxicity assays were performed in 96-well plates at a density of 1×10^5 cells/well. The lactate dehydrogenase (LDH) released by cells was detected using a Cytotox 96 kit (Promega, Madison, USA). All experiments were performed three times in duplicate.

Motility and biofilm formation assays

Strains were diluted to OD₆₀₀ 1.0, and then spotted on LBS medium containing 0.35% agar. The swimming ability was recorded by measuring the colony diameter after 12 h at 30°C. For biofilm formation assay, strains were cultured overnight at 30°C in 1% NaCl-LB broth. The cultures (50 μ L) were diluted in 5 mL LBS in glass tubes and incubated at 30°C without shaking for 72 h. The bacterial incubation was transferred to a clean cuvette and the optical density of was measured at 600 nm. Total biofilm formation was measured by 1% (w/v) crystal violet staining at room temperature for 30 min. Crystal violet that stained biofilm was solubilized with dimethylsulphoxide (DMSO) and then measured at an optical density of 570 nm using Multiskan Spectrum (Thermo Scientific, USA). Finally, we calculated the relative biofilm formation as $1000 \times OD_{570} / (OD_{600} \times V1 \times V2)$, where V1 was the volume of bacterial incubation and V2 was the volume of DMSO.

Data availability

The genome sequences of the *V. alginolyticus* strains sequenced in this study have been deposited at

GenBank/DDBJ/ENA under the BioProject ID no. PRJNA836558.

Results

Phylogeny and population structure of *V. alginolyticus*

The genome sizes of the 184 *V. alginolyticus* strains ranged from 5.00 (strains Va62, Va116, and Va119) to 5.86 Mb (strain UCD-9C), with an average of 5.20 Mb. The GC contents ranged from 44.2 mol% (strain UCD-9C) to 44.8 mol% (strain 2014V-1011), with an average of 44.56 mol%. Approximately 4344–5303 CDSs per genome were predicted (Supplementary Table S2 and Table S3). ANI calculation showed the vast majority of strains had ANI values between 98.13% and 100% compared with the *V. alginolyticus* type strain ATCC 17749^T (Supplementary Figure S1), which was greater than the species boundaries of 95%–96% [35].

Among the 184 *V. alginolyticus* genomes, the core genome size was estimated to be 3.1 Mb, with an average GC content of 46.02 mol%, which was slightly higher than the average of the 184 genomes (44.56 mol%). The core genome was searched against the COG database to infer gene functions. Aside from the core genes mainly related to the fundamental physiological activities and biological processes, eight mobile genetic elements (MGEs) related genes were also identified using RAST Annotation Server against the core genome sequences, including one integrase and seven phage/ prophage-related factors, which indicates that they were acquired early in the emergence of *V. alginolyticus* and that they are stable in the genome.

A total of 230,751 SNPs were identified in the *V. alginolyticus* core genome. Compared with the complete genome ATCC 17749^T as the reference sequence, the number of core genome SNPs (cgSNPs) ranged from 29,652 (strain Va46) to 34,424 (both strains Va109 and Va110). A phylogenetic tree was constructed based on the cgSNPs, and three major lineages could be inferred, named Lineage 1 (L1) to Lineage 3 (L3) (Figure 1(A)). L1 showed deeper evolutionary roots and contained more isolates (43.5%, 80/184), which indicated they were introduced into the local region earlier than the isolates in L2 and L3. The phylogenetic analysis showed that some of the strains from China seas (like the Yellow Sea and South China Sea) were clustered together. However, regardless of isolation region or isolation source, there was no clear correlation between single isolation source and evolutionary cluster found in the phylogenetic tree (Figure 1(B)). Therefore, the various *V. alginolyticus* strains showed substantial evolutionary differences in geographic distribution or host

source, indicating a high genetic diversity even in a local region.

We further divided the total genomic dataset into several hierarchical sub-datasets containing different numbers of genomes. In the first sub-dataset, we removed the same clone obtained from a single sampling to form a sub-dataset of 123 isolates for analysis of more refined population structure of *V. alginolyticus*. Hierarchical Bayesian clustering based the phylogenetic tree was reconstructed for these *V. alginolyticus* isolates, and SNP-based genotyping showed that, among the L1 strains, four sub-lineages (named L1.1, L1.2, L1.3, and L1.4, respectively) could be further differentiated. Both L2 and L3 were further divided into two sub-lineages each (Figure 2(A)).

Sub-dataset-2 contained 164 strains associated with marine habitats, with isolated sources including seawater, marine sediment, fishes, and seagrass. This sub-dataset, from which clinical and food-derived strains were removed, was ideal for characterizing the distribution of *V. alginolyticus* populations in marine ecological niches. Strains from Europe and North America showed a scattered distribution; for example, strains isolated from the USA were nested within the L1 and L2 population but clustered in different sub-lineages with restricted diversification (Figure 2(B)). The evolutionary tree indicated that, even for the same marine niche, *V. alginolyticus* populations did not show clear geographical aggregation. However, strains from Asia (mainly Chinese isolates) were found throughout in the L1, L2, and L3 lineages (Figure 2(B)). We speculated that the genetic diversity of *V. alginolyticus* may be related to some non-geographic separation factors, such as human activities.

To test this hypothesis, we then singled out 163 strains with well-defined isolation sites as a third sub-dataset. By calculating the genetic distance and the actual geographical distance among *V. alginolyticus* strains, we found that the L3 strains were more affected by non-geographic separation factors (Mantel statistic r : 0.1315, P = 0.083916, Figure 2(C)), whereas L1 and L2 were less affected (both had a Mantel statistic P = 0.000999, Figures 2(D) and (E)). This evidence suggested that the spread of L3 (mainly including strains isolated from Chinese territorial seas) was likely to be closely related to human activities, whereas L1 and L2 tended to be locally endemic and formed clonal complex groups.

Pan-genome diversification

All genome sequences were analysed by two-dimensional hierarchical clustering analysis based on the presence or absence of CDSs to preliminarily assess

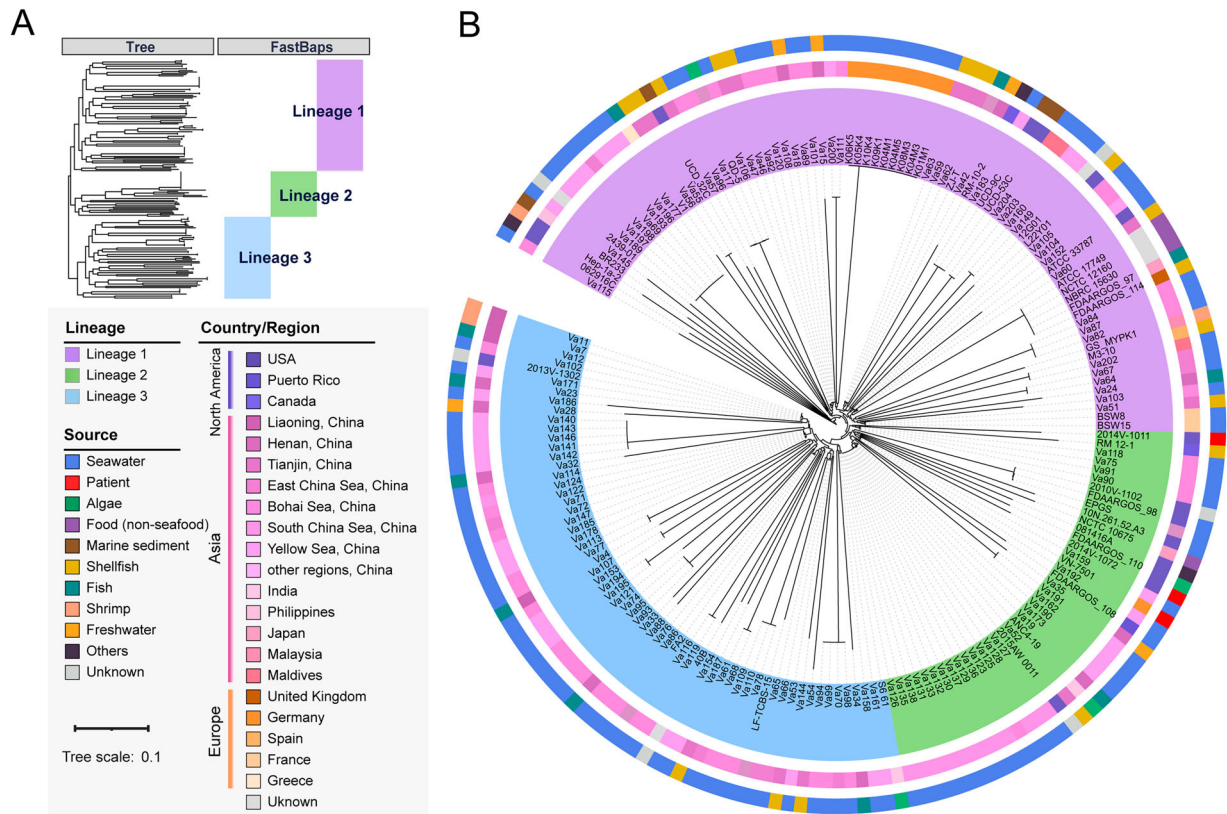


Figure 1. Population structure and phylogenetic analyses of *V. alginolyticus*. (A) Phylogenetic tree of *V. alginolyticus* constructed based on de-recombinational cgSNPs. Colours indicate the isolation region and host source of *V. alginolyticus* strains. Bootstrap values were calculated by 1000 replications. The horizontal bar indicates 0.1 estimated nucleotide substitutions per site. (B) Evolutionary tree divided into 3 main lineages using FastBaps R package with an optimized BAPS prior. Lineages 1–3 are indicated in purple, green and blue, respectively.

the consistency of these *V. alginolyticus* genomes. From a global perspective, there were certain differences in the genome composition of *V. alginolyticus*, and the geographical distribution was complex and diverse. Some strains from China territorial seas formed a separate cluster that distinguished strains from other regions, such as strains from the South China Sea and the Bohai Sea, whereas the strains from the Yellow Sea showed a multiple-clustering trend (Figure 3). In the Chinese Mainland, only the strains from Liaoning Province formed a single cluster, whereas the strains from Henan Province and Tianjin Municipality were scattered in various clusters. The same was true for the clustering of global strains. For example, several strains from Japan, Germany, France, and Maldives formed separate clusters despite a very limited number of strains and isolation sources; however, strains from other geographical locations, represented by the United States strains, were widely distributed, as highlighted in the arrows in Figure 3.

Next, to calculate the genomic differences of strains from different geographical origins, the core genome and accessory genome of these sequenced *V. alginolyticus* strains were analysed in depth.

Approximately 24,725 genes were predicted and annotated that were considered to be the pan-genome of the *V. alginolyticus* strains in this study (Figure S2A). The core-genome curve (Figure S2B) showed a flat slope, which indicated that it had achieved a full representation of this species core diversity. As the number of strains increased, the number of pan genes was growing rapidly while the number of the core genes gradually stabilized. Altogether there were 3323 (13.4%) genes identified as core genes ($99\% \leq \text{strains} \leq 100\%$), and the number of pan genes was equal to 7.4 times that of core genes. And there were also 422 soft core genes ($95\% \leq \text{strains} < 99\%$) in the pan-genome.

In addition, the analysis with protein identity set to 90% resulted in partial strains with similar accessory genome content gathering to form several groups, such as the three typical groups in the red box (Figure S2A), named Groups 1–3. Exploring the gene set that was exclusive for these three groups, 147 genes were found to be unique for and present in all nine isolates from the Kiel-Fjord, Germany in Group 1 (Supplementary Table S4). In the same way, 71 and 80 unique gene clusters were identified in Group 2 and Group 3, comprising

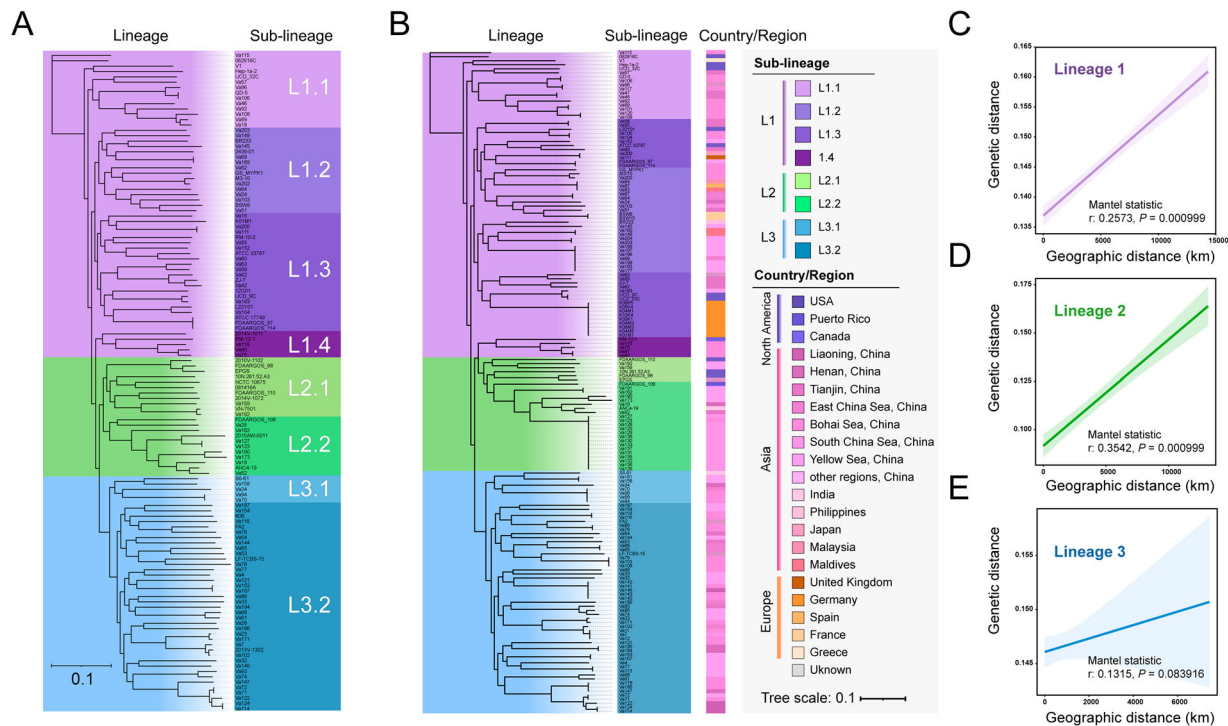


Figure 2. Phylogenetic analysis of three hierarchical sub-datasets containing different number of *V. alginolyticus*. (A) Phylogenetic tree of *V. alginolyticus* eliminated from a single sampling belonging to the same clonal group. (B) Phylogenetic tree constructed based on marine habitat-related strains. The colours indicate sublineages and isolation regions of *V. alginolyticus* strains. (C) Correlation analysis between genetic distance and geographical distances within L1 strains (Mantel statistic $r: 0.2573$, P value = 0.000999). (D) Correlation analysis between genetic distance and geographical distances within L2 strains (Mantel statistic $r: 0.3542$, P value = 0.000999). (E) Correlation analysis between genetic distance and geographical distances within L3 strains (Mantel statistic $r: 0.1315$, P value = 0.083916).

14 South China Sea-derived strains and 7 partial Yellow Sea-derived strains, respectively (Supplementary Tables S5 and S6). The annotation of these three groups remains incomplete because the majority of genes (more than 2/3) were only annotated as hypothetical proteins despite being mapped against the Gene Ontology (GO) database, Cluster of Orthologous Groups of proteins (COG), Kyoto Encyclopedia of Genes and Genomes (KEGG), and Swiss-Prot protein database. The annotation information for the remaining genes of Group 1 mainly included aspects of molecular function and biological process, and included the specific functions such as lipid transport and metabolism, transcription, energy production and conversion, and multi-drug resistance (Supplementary Table S4). The unique accessory genes of the strains from the South China Sea (Group 2) were mainly responsible for carbohydrate transport and metabolism, and cellular component organization or biogenesis (Supplementary Table S5). For partial Yellow Sea-derived strains (Group 3), the genes with more detailed functional information were involved in signal transduction and transport and metabolism (Supplementary Table S6). These accessory genome-related evidence reclassified *V. alginolyticus* as a relatively closer affinity, thereby indicating

substantial genomic differences with respect to other groups.

Distribution characteristics of virulence-related genes

Based on the annotation of the VFDB database via the relatively relax cutoff (identity $\geq 80\%$, length coverage $\geq 50\%$), the virulence components harboured by 184 *V. alginolyticus* strains were identified and categorized as 8 virulence-related classes involved in 14 virulence-related factors and 85 potential virulence genes (Table 1). The number of virulence genes carried by each strain ranged from 50 (strain Va52) to 88 (strain 062916C), with an average of 74 ± 4 (Supplementary Table S7). The functions of these virulence genes were identified as cell chemotaxis, motility, T3SS, haemolysin, lipopolysaccharide synthesis, and immune evasion. The positivity rate of virulence factors related to T3SS reached 99.5% (183/184) in these strains. It is worth mentioning that all *V. alginolyticus* strains carried the thermolabile haemolysin gene (*tlh*). Only one strain isolated from Canada, RM-12-1, carried the haemolysin *hlyD* gene (Supplementary Table S7).

Then we used a more conservative and stricter cutoff for protein sequence comparison.

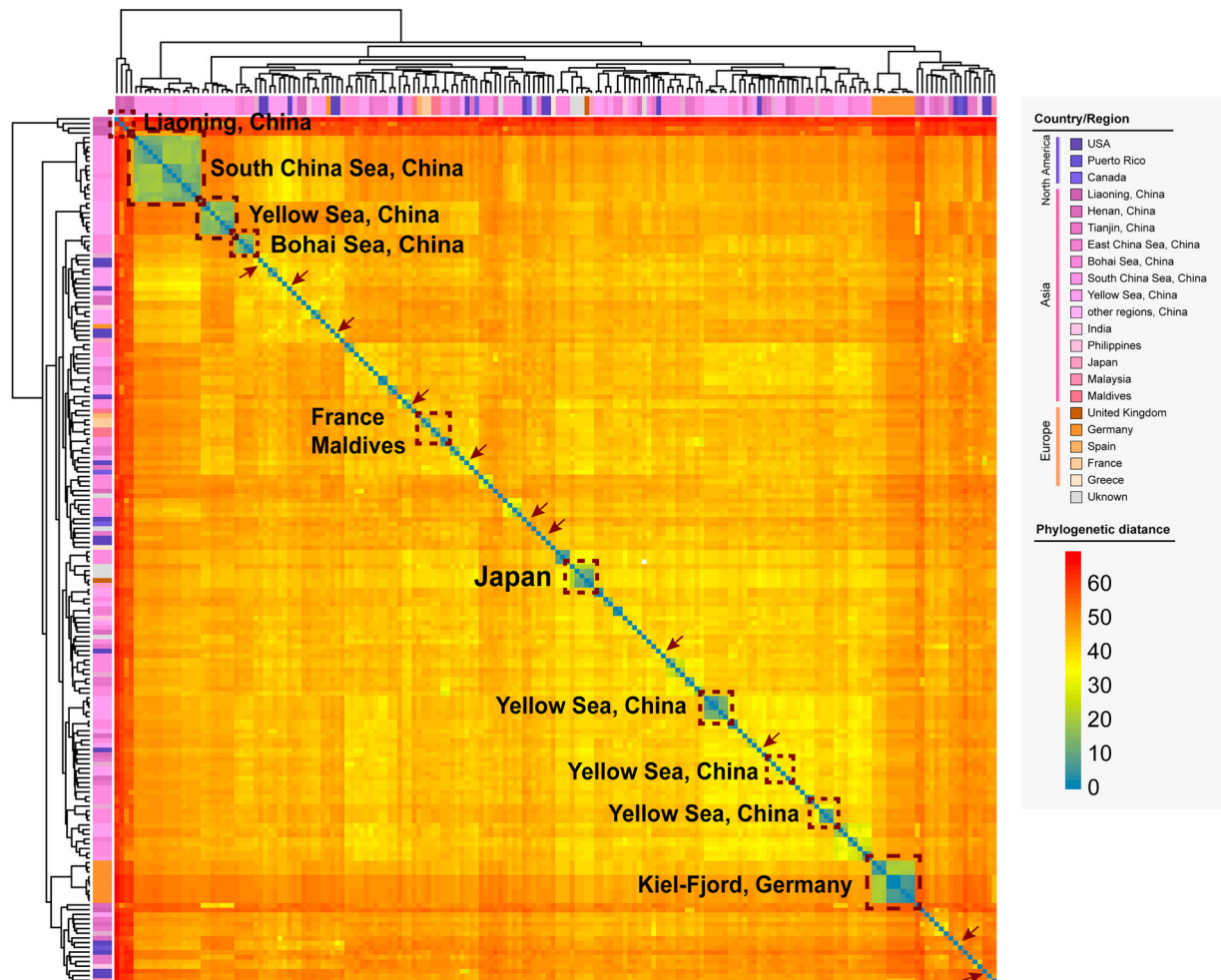


Figure 3. Two-dimensional hierarchical clustering based on the whole genome sequences of *V. alginolyticus*. Isolation regions or countries are presented in the corresponding dashed boxes, whereas strains from the USA are marked with brown arrows. Colours from blue to red represent increasing genomic distances.

Consequently, we identified 30 virulence genes with known functions (Figure 4(A)). All these *V. alginolyticus* strains had 8 highly conserved virulence genes, with the biological functions including thermolabile haemolysin (*tlh*), adherence factor (*VP1611*), and flagella synthesis and cell chemotaxis (*fliI*, *flhA*, *fleN*, *cheR*, *cheW*, *cheY*). The heatmap of virulence-related factors showed that most of the *V. alginolyticus* harboured almost an equal number of virulence genes, which indicated that these strains

shared a similar virulence spectrum (Figure 4(A)). An important finding was that there did not appear to be any clear distinctions in (potential) virulence determinants found in China vs. global isolates. By linking virulence-related genes with isolation regions or isolation hosts, no relevant distribution characteristics were observed between the *V. alginolyticus* strains.

Additionally, the genes of cholera toxin (*ctxA/ctxB*) of *V. cholerae* O1/O139, thermostable direct

Table 1. Function and pathogenic role of the virulence factors of *Vibrio alginolyticus*.

VFclass	Virulence factors	Function or Pathogenic Role
Adherence	Multivalent adhesion molecule	Cell-cell adhesion
Chemotaxis and motility	Flagella	Flagellum biogenesis, motor activity, pathogenesis
Quorum sensing	Autoinducer-2	Autoinducer synthesis, quorum sensing
Secretion system	T3SS1	Translocated effector, protein secretion
	T6SS	T6SS structural component
	T4SS	T4SS effector
Toxin	Haemolysin/cytolysin	Protein transport, pathogenesis
	Thermolabile haemolysin	Lipid metabolic process, pathogenesis
Endotoxin	LOS	Multifunctional enzyme
	LPS	Lipopolysaccharide biosynthesis
Immune evasion	Capsule	Polysaccharide biosynthesis, chemotaxis
	immunogenic lipoprotein	Membrane component
Others	O-antigen	Lipopolysaccharide biosynthesis
	elongation factor	Protein biosynthesis

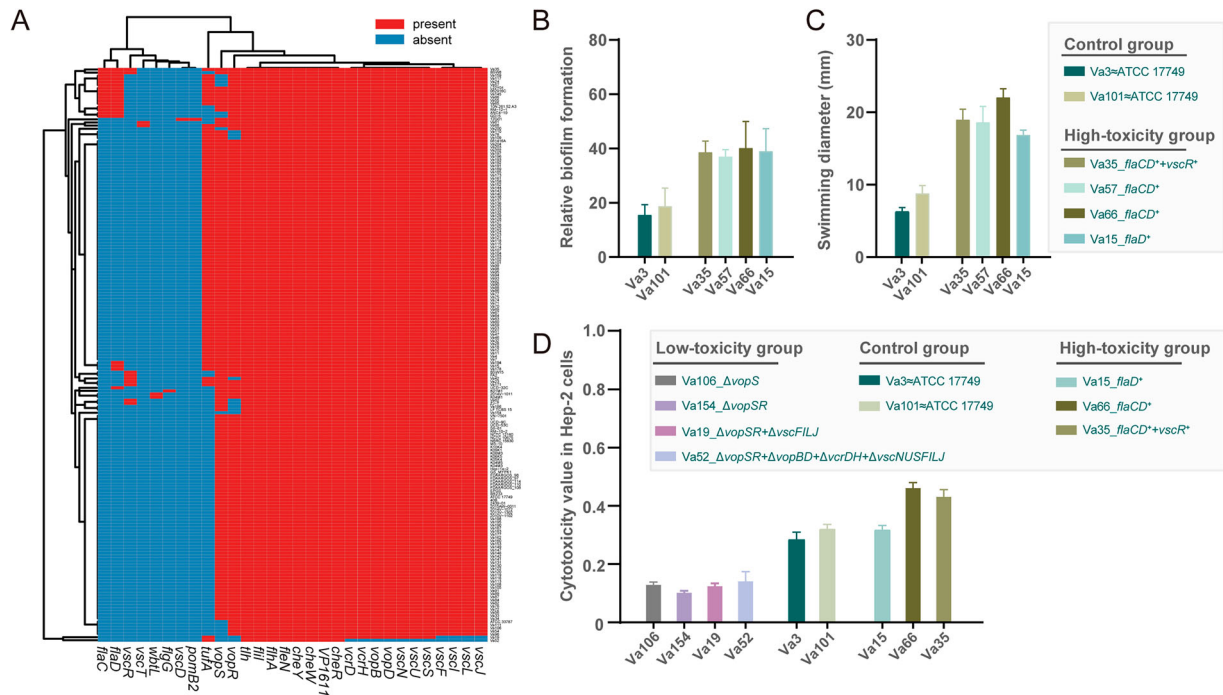


Figure 4. Virulence analysis of *V. alginolyticus*. (A) Heatmap for virulence-related factors of *V. alginolyticus*. Red represents the presence of genes, while blue represents the absence of genes. (B) Relative biofilm formation of six representative strains. The vertical coordinate represents the relative amount of biofilm formation measured by 1% (w/v) crystal violet (w/v) staining. (C) Swimming ability of six representative strains. The vertical coordinate represents the colony diameter after 12 h of incubation. Strains Va3 and Va101 were selected as the control group based on the same virulence spectrum to ATCC 17749^T, the type strain of *V. alginolyticus*. In the high-toxicity group, four strains (Va15, Va35, Va57, and Va66) with 1–3 additional *flaC* (flagella), *flaD* (flagella), and *vscR* (T3SS) genes were compared with ATCC 17749^T. (D) Cytotoxicity values of nine representative strains. Higher values indicate higher cytotoxicity. The high-toxicity group and the control group were as described above. For the low-toxicity group, compared with ATCC 17749^T, another four strains (Va19, Va52, Va106, and Va154) were chosen with natural deletion of one or more virulence genes (the gene family including *vopSR*, *vopBD*, *vcrDH*, and *vscNUSFILJ*).

haemolysin (*tdh*) and TDH related haemolysin (*trh*) of *V. parahaemolyticus* were not detected. The thermolabile haemolysin gene (*tlh*) was subsequently compared

with the reference sequence *V. parahaemolyticus* ATCC 33846 (GenBank accession No.: GU971655.1). Sequence comparison showed that the DNA sequence

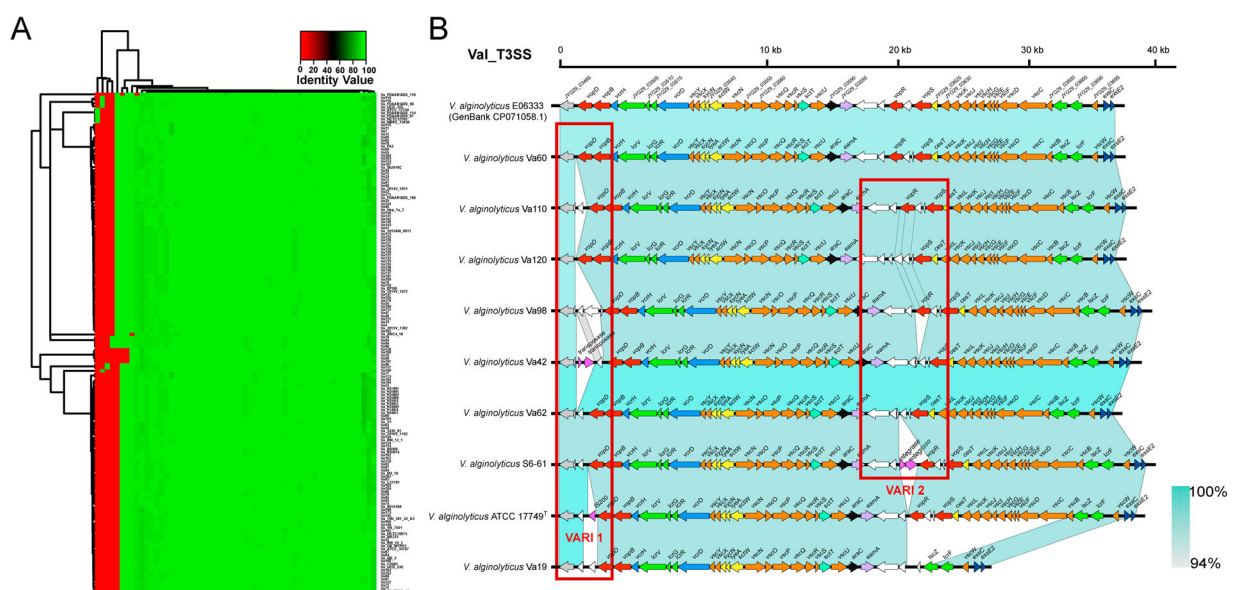


Figure 5. Type III secretion system of *V. alginolyticus*. (A) Heatmap for 165 available T3SS sequences. Red indicates low identity values, whereas green indicates high identity values. (B) Gene cluster distribution of five different T3SS genotypes in *V. alginolyticus*. The two identified variable regions (VARI1 and VARI2) are marked with red boxes. The colours represent different gene families, and the length of the arrow indicates the size of each CDS.

similarity was 84.6% – 85.7%, but the amino acid sequence similarity reached 92.8% – 93.7%. The *tlh* gene sequences were used to construct the split network tree (Supplementary Figure S3). Consequently, the *tlh* gene carried by *V. alginolyticus* is likely to have contributed to pathogenicity because it encoded a phospholipase A2 protein in *V. parahaemolyticus* when its expression was upregulated under conditions mimicking the human intestine [36,37]. Moreover, it was found that the *cheR* gene sequence NJ tree roughly classified these *V. alginolyticus* isolates into four groups (Supplementary Figure S4).

Subsequently, the strains in the high-toxicity group had flagella-related genes (*flaCD*) exhibiting superior biofilm formation ability and swimming motility compared with the control group (Figures 4(B) and (C)). In addition, we also selected four representative strains missing the T3SS-related *vopBDSR* and *vscNUSFILJ* genes as the low-toxicity group. Strains lacking *vopS* showed a significant reduction in cytotoxic infectivity (Figure 4(D)). Genes such as *vopBDR* and *vscNUSFILJ* had minimal impact on cytotoxicity, whereas *flaCD* genes enhanced cytotoxic effects (Figure 4(D)).

Type III secretion system

Numerous T3SS-associated genes were identified in this study. T3SS was of particular interest, and there were indeed some doubts about the distribution and composition of T3SS in *V. alginolyticus*. First, T3SS was initially identified by the potential T3SS segment composed of CDSs. As a result, we obtained a total of 165 positive T3SS sequences from each genome (the remaining 19 incomplete T3SS sequences were discarded). Then, all the potential T3SS sequences were manually checked and determined based on the locus of these segments and the existence of known conserve genes of T3SS.

After an extraction of each CDS in the T3SS sequences, a clustering heatmap based on comparison of the similarity of each CDS was constructed (Figure 5(A)). According to the identified CDS arrangement, these T3SS sequences could be classified into five subtypes. The subtype represented by strain Va110 accounted for the highest proportion (76/165, 46.1%), followed by the subtype represented by Va60 (75/165, 45.5%). The remaining three subtypes only appeared in a few strains. Among them, the acquired sequence length ranged from 36,924 to 38,742 bp with the variant number of CDSs ranging from 46 to 50. The annotation information of the five types of T3SS gene clusters is presented in Supplementary Table S8. The CDS components of these five T3SS types were presented in Figure 5(B). Their backbone had a similar structure, but there were two variable regions in the red box representing some small differences involving one to four CDSs, due to the inserted

Table 2. Distribution and positive rate of antibiotic resistance genes.

Class of antibiotics	Genotype	Number of strains	Positive rate (%)
β-lactams	<i>bla</i> _{CARB-42}	184	100
Quinolones	<i>qnrVC5</i>	1	0.5
Aminoglycosides	<i>aph(3'')-Ia,aph(3'')-Ib,aph(6)-Id</i>	9	4.9
Sulphonamides	<i>dfrA15,dfrA31,sul1,sul2</i>	11	6.0
Amido alcohols	<i>floR</i>	7	3.8

sequence (i.e. IS200 in the T3SS of *V. alginolyticus* ATCC 17749^T) or other genetic events (i.e. the deletion or insertion of several hypothetical proteins).

Antibiotic resistance genes

We found that five classes of antibiotic resistance-related genes were present in the *V. alginolyticus* genomes (Table 2), named β-lactams (*bla*_{CARB-42}), quinolones (*qnrVC5*), aminoglycosides [*aph(3'')-Ia, aph(3'')-Ib, aph(6)-Id*], sulphonamides (*dfrA15, dfrA31, sul1, sul2*), and amide alcohols (*floR*). Among them, the prevalence of β-lactam resistance genes was 100% and included a single genotype (*bla*_{CARB-42}). This finding indicated that *V. alginolyticus* may be naturally resistant to β-lactam drugs. The sulphonamide resistance genes ranked secondly and were distributed in 11 of 184 strains (6.0%). When considering multi-drug resistance, only a handful of strains ($n = 11$, 6.0%) carried multiple drug resistance genes. For example, the strain ZJ-T from China carried four different kinds of resistance genes, and it had carried the largest number of resistance genes. Further investigation revealed that these drug-resistance genes of strain ZJ-T were located in a large gene cluster on the same scaffold. After comparison with the BLASTn tool, this fragment was very similar to the integrated conjugative elements (ICEs, ICEVal056-1, accession No.: KR231688.1) of *V. alginolyticus*, with coverage and identity of 70% and 99.98%, respectively. This indicated that the strain ZJ-T may have obtained a large fragment carrying multiple drug-resistance genes through HGT.

Discussion

A variety of marine microorganisms can spread across oceans, such as in the case of the global spread of pathogenic clones of *V. parahaemolyticus* and *V. cholerae*. However, human activity is an important factor in the spread of these pathogenic clones. For example, human activity is associated with a cholera outbreak in Haiti [38]. We still do not have a clear understanding of the divergence, prevalence, and spread of *V. alginolyticus*. In this study, comparative genomic analysis has revealed several different dimensions of evolutionary characteristics in *V. alginolyticus*

genomes on the basis of a systematic description of the population structure features for 184 isolates from different regions and sources and investigation of the distribution of virulence genes and drug resistance in the *V. alginolyticus* strains.

Pan-genome analysis helps us understand the core-/pan-genes and unique gene clusters of this species, whereas the core genome is usually composed of essential genes, such as those that encode for the major redox reactions [39]. The accessory genome was found to be related to *V. alginolyticus* niche adaptation and biological characteristics, including genes related to virulence and drug resistance. The number of pan-genes was equal to 7.4 times that of the core genes from the pan-genome analysis (Figure 4(A,B)); this indicates that *V. alginolyticus* had a strong adaptability to the external environment and the variable host habitats, with a rich and diverse pan gene pool. Based on these results, it is speculated that human activities, such as shipping, tourism, and global-seafood trade, may promote to transoceanic transmission of *V. alginolyticus* in seawater. This allows strains in different sea areas to frequently exchange genes (e.g. HGT mediated by MGEs [40]), which ultimately affects the *V. alginolyticus* population structure and evolution. For example, the *V. alginolyticus* strains from the Kiel-Fjord (Germany) have evolved from clonal expansion following HGT-driven niche-adaptation [25].

The phylogenetic tree based on the cgSNPs provided a clear interpretation of the evolutionary relationship between 184 *V. alginolyticus* strains. It is generally accepted that strains in the same clade are more closely related to each other and may have a common evolutionary ancestor. However, the phylogenetic tree (Figure 1) showed that *V. alginolyticus* were classified into the same clade and were isolated from different times and different geographic regions. The strains Va115, 062916C, and Hep-1a-2 formed a single evolutionary branch respectively, which was distinct from other strains, and these strains were ancient from an evolutionary perspective. This finding indicates that the *V. alginolyticus* isolated from China and the USA between 2014 and 2016 had evolved and spread. We used a hierarchical Bayesian clustering algorithm implemented in fastBAPS. It helped to split phylogenetic trees into three lineages and eight sublineages (Figures 1 and 2) using a population genomic model. We further divided the total genomic dataset of *V. alginolyticus* into three sub-datasets. However, because of the uneven number of strains in the isolation area, the isolation region of *V. alginolyticus* did not cover the global geographic location well, which posed a challenge for analysing the global population structure.

The core genome evolutionary relationships were not completely consistent with those of the pan-

genome. The accessory genes in bacteria may have been derived in different stages of evolution in order to adapt to various hard-condition living situations, the accessory genome plays an inescapable role in evolution of *V. alginolyticus* for its environmental adaptability. The phylogenetic tree not only appeared little interspecies relation between *V. alginolyticus* strains isolated from different host sources and geographical regions but indicated that there was a highly genetic diversity among the strains.

The creatures that inhabit the Earth can fully utilize resources if there is not any competition or other predators. However, because of the existence of interspecies competition, what a creature can occupy is nothing but the ecological niche within the scope of viability [41,42]. Over a long period of time, bacteria have evolved a competition mechanism to compete for limited resources, which included the evolution of virulence genes and antibiotic resistance genes. This mechanism allows *Vibrio* species to infect humans and aquatic animals, and to expand their ecological niches. This study found that there was a rich diversity of virulence factors in *V. alginolyticus* populations, which are mainly associated with chemotaxis, motility, and secretion system. Consistent with a previous study [43], more than 100 acetylation-modified proteins were predicted as virulence factors in *V. alginolyticus*. Another study in Mexico found that several genes encoding virulence factors were present in environmental strains of *V. alginolyticus*, including *tdh*, *proA*, *wza*, *vopD*, *hcp*, *vasH* and *vgrG* genes [44].

Additionally, flagella-related genes (like *fleN*, *flhA*, *fliL*) have roles in flagellum biogenesis and motor activity, which have been proven to be closely related to biological and cellular processes such as chemotaxis, biofilm formation, and colonization for bacteria of the genus *Vibrio* [21,45,46]. As for *cheW* gene, an important downstream gene in the bacterial chemotaxis pathway, was composed of *V. cholerae* chemotaxis cluster III system which was regulated by RpoS and quorum sensing in response to polar localization [47]. *V. parahaemolyticus* RIMI 2210633 possesses two sets of T3SSs on chromosomes 1 and 2, designated T3SS1 and T3SS2, respectively [48]. Likewise, *V. alginolyticus* required its T3SS to cause rapid death of infected host cells such as fish and shrimp, and the T3SS is a highly conserved apparatus among these *V. alginolyticus* strains (Figure 5).

Many other studies have explored the infection mechanism of T3SS in *V. alginolyticus* [49,50]; it can deliver the effectors directly into cells of hosts across bacterial and host membranes. *Vibrio* T3SS initiates a multifaceted process leading to the death of mammalian cell lines, starting with autophagy, followed by cell rounding, and culminating in caspase-independent cell death [51,52]. The effector protein VopS plays a crucial role in inducing cell rounding and

disrupting the actin cytoskeleton by inhibiting Rho GTPases [53]. Zhao et al. demonstrated that VopS from *V. alginolyticus* not only contributes to fish cell rounding through Rho GTPase inhibition but also plays an essential role in apoptosis induction. A deletion mutant lacking VopS exhibited severe impairment in its ability to induce these two cellular responses, whereas transfection of VopS into the fish cell line FHM alone is sufficient to trigger both cell rounding and apoptosis [50]. Those findings are consistent with the results of this study.

There is currently a lack of worldwide surveillance information regarding *V. alginolyticus* infections, as this pathogen is not taken seriously in many countries, which probably underestimate the clinical infectivity of this pathogen. Unfortunately, our efforts to link the virulence factors to the isolation sources under a variety of conditions have been unsuccessful. The divergence of virulence genes among environmental strains is so subtle that the minimal variation in a certain virulence gene sequence or SNP-based locus is not powerful enough to establish the relationship between strains and pathogenicity. Therefore, the pathogenicity of *V. alginolyticus* may be affected by multiple factors. The pathogenicity may depend on the complex interaction among the multiplexing systems, such as the host species, the host's niche, and the pathogenic bacteria itself.

Nowadays, exposure to seawater environments through recreational (e.g. surfing, snorkelling, speed boating, jet skiing) or occupational activities (e.g. sailing, crabbing, fishing) increases the risk of disease caused by *V. alginolyticus*, especially when an individual's immunity is weak. This suggests that *V. alginolyticus* is a foundational condition rather than a decisive factor for human diseases, and the pathogenic progress may be accelerated and deteriorated by the synergistic effect of multiple factors. The functions of these potential virulence genes deserve more attention.

The formation of flagella confers motility to bacteria, enabling them to colonize both abiotic and biotic surfaces, optimize growth and survival, and evade desiccation in hostile host environments. *Vibrio* genomes harbour five or six polar flagellin genes located at two distinct genomic locations [54]. The expression of these genes are tightly linked to *Vibrio* virulence and host colonization [55]. Mutation in *flaC* within *V. vulnificus* leads to a significant reduction in motility, adhesion, and cytotoxicity [56]. Mobley et al. introduced a nonpolar mutation into the *flaD* gene and evaluated its impact on virulence *in vivo*. The *hpmA flaD* mutant exhibited approximately 100-fold lower recovery compared with the *hmpA* mutant or wild-type parent strain, which indicates clear attenuation of virulence potential [57].

More importantly, several studies have demonstrated that the antibiotic resistance genes are physically linked to MGEs and could potentially propagate to other bacterial species through HGT [58]. We found that 184 strains all carried the β -lactam resistance gene *bla*_{CARB-42}; therefore, *V. alginolyticus* may be naturally resistant to β -lactam drugs. Similarly, another study also found that more than 90% of the *V. alginolyticus* strains were resistant to β -lactams antibiotics, and other antibiotics including cephalotin, amikacin, cephalexin and pefloxacin [44]. Another survey in Korea showed that *V. alginolyticus* isolates were mainly resistant to ampicillin, vancomycin, and cephalothin [59]. In our study, the only strain ZJ-T (one out of 184 strains), isolated from diseased *Epinephelus coioides* in Guangdong Province, China [60], could serve as a representative with carrying several potential drug resistance genes. However, another study found that the prevalence of multi-resistance to four or more antimicrobials in *V. alginolyticus* (11.1%) was higher than that in *V. parahaemolyticus* (5%) [61]. Overall, these investigations of *V. alginolyticus* antimicrobial resistance should play an early-warning role in *V. alginolyticus* monitoring and treatment of clinical infection.

Our comprehensive analyses of *V. alginolyticus* genomes have further enhanced the understanding of their virulence factors, drug resistance genes, population structure and evolutionary characters. We demonstrated the detailed genetic diversity of the *V. alginolyticus* genomes. This study provided a framework for systematic characterization of the *V. alginolyticus* genomes, which may be broadly applicable to diverse *Vibrionaceae* microorganisms and amenable to comparative analysis.

Acknowledgements

We thank Mallory Eckstut, PhD, from Liwen Bianji (Edanz) for editing the English text of a draft of this manuscript.

Disclosure statement

No potential conflict of interest was reported by the author(s).

Funding

This work was supported by the National Science and Technology Major Project (2018ZX10714002, 2017ZX10303405-002).

References

- [1] Grimes DJ. The vibrios: scavengers, symbionts, and pathogens from the Sea. *Microb Ecol.* 2020;80(3):501–506. doi:10.1007/s00248-020-01524-7
- [2] Rockstroh T. [Changes in the nomenclature of bacteria after the 8th edition of Bergey's Manual of the

- Determinative Bacteriology]. Z Arztl Fortbild (Jena). 1977;71(11):545–550.
- [3] Baker-Austin C, Oliver JD, Alam M, et al. *Vibrio* spp. infections. Nat Rev Dis Primers. 2018;4(1):8. doi:10.1038/s41572-018-0005-8
- [4] Feingold MH, Kumar ML. Otitis media associated with *Vibrio alginolyticus* in a child with pressure-equalizing tubes. Pediatr Infect Dis J. 2004;23(5):475–476. doi:10.1097/01.inf.0000126592.19378.30
- [5] Howard RJ, Pessa ME, Brennaman BH, Ramphal R (1985) Necrotizing soft-tissue infections caused by marine vibrios. Surgery 98(1):126–130.
- [6] Jacobs Slifka KM, Newton AE, Mahon BE. *Vibrio alginolyticus* infections in the USA, 1988–2012. Epidemiol Infect. 2017;145(7):1491–1499. doi:10.1017/S0950268817000140
- [7] Janda JM, Powers C, Bryant RG, et al. Current perspectives on the epidemiology and pathogenesis of clinically significant *Vibrio* spp. Clin Microbiol Rev. 1988;1(3):245–267. doi:10.1128/CMR.1.3.245
- [8] Wang Q, Ji W, Xu Z. Current use and development of fish vaccines in China. Fish Shellfish Immunol. 2020;96:223–234. doi:10.1016/j.fsi.2019.12.010
- [9] Ruwandeepika HA, Defoirdt T, Bhowmick PP, et al. In vitro and in vivo expression of virulence genes in *Vibrio* isolates belonging to the Harveyi clade in relation to their virulence towards gnotobiotic brine shrimp (*Artemia franciscana*). Environ Microbiol. 2011;13(2):506–517. doi:10.1111/j.1462-2920.2010.02354.x
- [10] Oberbeckmann S, Wichels A, Maier T, et al. A polyphasic approach for the differentiation of environmental *Vibrio* isolates from temperate waters. FEMS Microbiol Ecol. 2011;75(1):145–162. doi:10.1111/j.1574-6941.2010.00998.x
- [11] Kuang SF, Xiang J, Chen YT, et al. Exogenous pyruvate promotes gentamicin uptake to kill antibiotic-resistant *Vibrio alginolyticus*. Int J Antimicrob Agents. 2024;63(1):107036. doi:10.1016/j.ijantimicag.2023.107036
- [12] Zhou K, Tian KY, Liu XQ, et al. Characteristic and otopathogenic analysis of a *Vibrio alginolyticus* strain responsible for chronic otitis externa in China. Front Microbiol. 2021;12:750642. doi:10.3389/fmicb.2021.750642
- [13] Gu D, Liu H, Yang Z, et al. Chromatin immunoprecipitation sequencing technology reveals global regulatory roles of low-cell-density quorum-sensing regulator AphA in the pathogen *Vibrio alginolyticus*. J Bacteriol. 2016;198(21):2985–2999. doi:10.1128/JB.00520-16
- [14] Wu C, Zhao Z, Liu Y, et al. Type III secretion 1 effector gene diversity among *Vibrio* isolates from coastal areas in China. Front Cell Infect Microbiol. 2020;10:301. doi:10.3389/fcimb.2020.00301
- [15] Sheng L, Lv Y, Liu Q, et al. Connecting type VI secretion, quorum sensing, and c-di-GMP production in fish pathogen *Vibrio alginolyticus* through phosphatase PppA. Vet Microbiol. 2013;162(2–4):652–662. doi:10.1016/j.vetmic.2012.09.009
- [16] Huang Z, Yu K, Fang Y, et al. Comparative genomics and transcriptomics analyses reveal a unique environmental adaptability of *Vibrio fujianensis*. Microorganisms. 2020;8(4):555.
- [17] Montieri S, Suffredini E, Ciccozzi M, et al. Phylogenetic and evolutionary analysis of *Vibrio parahaemolyticus* and *Vibrio alginolyticus* isolates based on *toxR* gene sequence. New Microbiol. 2010;33(4):359–372.
- [18] Yingkajorn M, Sermwitayawong N, Palittapongarnpim P, et al. *Vibrio parahaemolyticus* and its specific bacteriophages as an indicator in cockles (*Anadara granosa*) for the risk of *V. parahaemolyticus* infection in Southern Thailand. Microb Ecol. 2014;67(4):849–856. doi:10.1007/s00248-014-0382-9
- [19] Salamone M, Nicosia A, Ghersi G, et al. *Vibrio* proteases for biomedical applications: modulating the proteolytic secretome of *V. alginolyticus* and *V. parahaemolyticus* for improved enzymes production. Microorganisms. 2019;7(10):387.
- [20] Zhu S, Nishikino T, Hu B, et al. Molecular architecture of the sheathed polar flagellum in *Vibrio alginolyticus*. Proc Natl Acad Sci U S A. 2017;114(41):10966–10971. doi:10.1073/pnas.1712489114
- [21] Khan F, Tabassum N, Anand R, et al. Motility of *Vibrio* spp.: regulation and controlling strategies. Appl Microbiol Biotechnol. 2020;104(19):8187–8208. doi:10.1007/s00253-020-10794-7
- [22] Echazarreta MA, Klose KE. *Vibrio* flagellar synthesis. Front Cell Infect Microbiol. 2019;9:131. doi:10.3389/fcimb.2019.00131
- [23] Liu XF, Cao Y, Zhang HL, et al. Complete genome sequence of *Vibrio alginolyticus* ATCC 17749 T. Genome Announc. 2015;3(1):45–47.
- [24] Wang P, Wen Z, Li B, et al. Complete genome sequence of *Vibrio alginolyticus* ATCC 33787(T) isolated from seawater with three native megaplasmids. Mar Genomics. 2016;28:45–47. doi:10.1016/j.margen.2016.05.003
- [25] Chibani CM, Roth O, Liesegang H, et al. Genomic variation among closely related *Vibrio alginolyticus* strains is located on mobile genetic elements. BMC Genomics. 2020;21(1):354. doi:10.1186/s12864-020-6735-5
- [26] Bankevich A, Nurk S, Antipov D, et al. SPAdes: a new genome assembly algorithm and its applications to single-cell sequencing. J Comput Biol. 2012;19(5):455–477. doi:10.1089/cmb.2012.0021
- [27] Gurevich A, Saveliev V, Vyahhi N, et al. QUAST: quality assessment tool for genome assemblies. Bioinformatics. 2013;29(8):1072–1075. doi:10.1093/bioinformatics/btt086
- [28] Hyatt D, Chen GL, Locascio PF, et al. Prodigal: prokaryotic gene recognition and translation initiation site identification. BMC Bioinformatics. 2010;11:119. doi:10.1186/1471-2105-11-119
- [29] Seemann T. Prokka: rapid prokaryotic genome annotation. Bioinformatics. 2014;30(14):2068–2069. doi:10.1093/bioinformatics/btu153
- [30] Richter M, Rosselló-Móra R. Shifting the genomic gold standard for the prokaryotic species definition. Proc Natl Acad Sci U S A. 2009;106(45):19126–19131. doi:10.1073/pnas.0906412106
- [31] Page AJ, Cummins CA, Hunt M, et al. Roary: rapid large-scale prokaryote pan genome analysis. Bioinformatics. 2015;31(22):3691–3693. doi:10.1093/bioinformatics/btv421
- [32] Fu L, Niu B, Zhu Z, et al. CD-HIT: accelerated for clustering the next-generation sequencing data. Bioinformatics. 2012;28(23):3150–3152. doi:10.1093/bioinformatics/bts565

- [33] Croucher NJ, Page AJ, Connor TR, et al. Rapid phylogenetic analysis of large samples of recombinant bacterial whole genome sequences using Gubbins. *Nucleic Acids Res.* 2015;43(3):e15. doi:10.1093/nar/gku1196
- [34] Tonkin-Hill G, Lees JA, Bentley SD, et al. Fast hierarchical Bayesian analysis of population structure. *Nucleic Acids Res.* 2019;47(11):5539–5549. doi:10.1093/nar/gkz361
- [35] Jain C, Rodriguez RL, Phillippy AM, et al. High throughput ANI analysis of 90 K prokaryotic genomes reveals clear species boundaries. *Nat Commun.* 2018;9(1):5114. doi:10.1038/s41467-018-07641-9
- [36] Klein SL, Gutierrez West CK, Mejia DM, et al. Genes similar to the *Vibrio parahaemolyticus* virulence-related genes *tdh*, *tlh*, and *vscC2* occur in other vibriaceae species isolated from a pristine estuary. *Appl Environ Microbiol.* 2014;80(2):595–602. doi:10.1128/AEM.02895-13
- [37] Broberg CA, Calder TJ, Orth K. *Vibrio parahaemolyticus* cell biology and pathogenicity determinants. *Microbes Infect.* 2011;13(12-13):992–1001. doi:10.1016/j.micinf.2011.06.013
- [38] Lantagne D, Balakrish Nair G, Lanata CF, et al. The cholera outbreak in Haiti: where and how did it begin? *Curr Top Microbiol Immunol.* 2014;379:145–164.
- [39] Falkowski PG, Fenchel T, Delong EF. The microbial engines that drive Earth's biogeochemical cycles. *Science.* 2008;320(5879):1034–1039. doi:10.1126/science.1153213
- [40] Aminov RI. Horizontal gene exchange in environmental microbiota. *Front Microbiol.* 2011;2:158. doi:10.3389/fmicb.2011.00158
- [41] Nicholson E, Keith DA, Wilcove DS. Assessing the threat status of ecological communities. *Conserv Biol.* 2009;23(2):259–274. doi:10.1111/j.1523-1739.2008.01158.x
- [42] Harrisson KA, Pavlova A, Gonçalves da Silva A, et al. Scope for genetic rescue of an endangered subspecies through re-establishing natural gene flow with another subspecies. *Mol Ecol.* 2016;25(6):1242–1258. doi:10.1111/mec.13547
- [43] Pang H, Li W, Zhang W, et al. Acetylome profiling of *Vibrio alginolyticus* reveals its role in bacterial virulence. *J Proteomics.* 2020;211:103543. doi:10.1016/j.jprot.2019.103543
- [44] Hernández-Robles MF, Álvarez-Contreras AK, Juárez-García P, et al. Virulence factors and antimicrobial resistance in environmental strains of *Vibrio alginolyticus*. *Int Microbiol.* 2016;19(4):191–198.
- [45] Syed KA, Beyhan S, Correa N, et al. The *Vibrio cholerae* flagellar regulatory hierarchy controls expression of virulence factors. *J Bacteriol.* 2009;191(21):6555–6570. doi:10.1128/JB.00949-09
- [46] Takekawa N, Isumi M, Terashima H, et al. Structure of vibrio FliL, a new stomatin-like protein that assists the bacterial flagellar motor function. *mBio.* 2019;10(2):e00292–19.
- [47] Ringgaard S, Hubbard T, Mandlik A, et al. RpoS and quorum sensing control expression and polar localization of *Vibrio cholerae* chemotaxis cluster III proteins in vitro and in vivo. *Mol Microbiol.* 2015;97(4):660–675. doi:10.1111/mmi.13053
- [48] Makino K, Oshima K, Kurokawa K, et al. Genome sequence of *Vibrio parahaemolyticus*: a pathogenic mechanism distinct from that of *V. cholerae*. *Lancet.* 2003;361(9359):743–749. doi:10.1016/S0140-6736(03)12659-1
- [49] Zhao Z, Chen C, Hu CQ, et al. The type III secretion system of *Vibrio alginolyticus* induces rapid apoptosis, cell rounding and osmotic lysis of fish cells. *Microbiology (Reading).* 2010;156(Pt 9):2864–2872. doi:10.1099/mic.0.040626-0
- [50] Zhao Z, Liu J, Deng Y, et al. The *Vibrio alginolyticus* T3SS effectors, Val1686 and Val1680, induce cell rounding, apoptosis and lysis of fish epithelial cells. *Virulence.* 2018;9(1):318–330. doi:10.1080/21505594.2017.1414134
- [51] Burdette DL, Yarbrough ML, Orvedahl A, et al. *Vibrio parahaemolyticus* orchestrates a multifaceted host cell infection by induction of autophagy, cell rounding, and then cell lysis. *Proc Natl Acad Sci U S A.* 2008;105(34):12497–12502. doi:10.1073/pnas.0802773105
- [52] Burdette DL, Yarbrough ML, Orth K. Not without cause: *Vibrio parahaemolyticus* induces acute autophagy and cell death. *Autophagy.* 2009;5(1):100–102. doi:10.4161/auto.5.1.7264
- [53] Yarbrough ML, Li Y, Kinch LN, et al. AMPylation of Rho GTPases by *Vibrio* VopS disrupts effector binding and downstream signaling. *Science.* 2009;323(5911):269–272. doi:10.1126/science.1166382
- [54] McCarter LL. Polar flagellar motility of the Vibrionaceae. *Microbiol Mol Biol Rev.* 2001;65(3):445–462. table of contents. doi:10.1128/MMBR.65.3.445-462.2001
- [55] Jung YC, Lee MA, Kim HS, et al. Role of DegQ in differential stability of flagellin subunits in *Vibrio vulnificus*. *NPJ Biofilms Microbiomes.* 2021;7(1):32. doi:10.1038/s41522-021-00206-7
- [56] Liang H, Xia L, Wu Z, et al. Expression, characterization and immunogenicity of flagellin FlaC from *Vibrio alginolyticus* strain HY9901. *Fish Shellfish Immunol.* 2010;29(2):343–348. doi:10.1016/j.fsi.2010.04.003
- [57] Mobley HL, Belas R, Lockett V, et al. Construction of a flagellum-negative mutant of *Proteus mirabilis*: effect on internalization by human renal epithelial cells and virulence in a mouse model of ascending urinary tract infection. *Infect Immun.* 1996;64(12):5332–5340. doi:10.1128/iai.64.12.5332-5340.1996
- [58] Verma J, Bag S, Saha B, et al. Genomic plasticity associated with antimicrobial resistance in *Vibrio cholerae*. *Proc Natl Acad Sci U S A.* 2019;116(13):6226–6231. doi:10.1073/pnas.1900141116
- [59] Kang CH, Shin Y, Jang S, et al. Antimicrobial susceptibility of *Vibrio alginolyticus* isolated from oyster in Korea. *Environ Sci Pollut Res Int.* 2016;23(20):21106–21112. doi:10.1007/s11356-016-7426-2
- [60] Chang C, Jin X, Chaoqun H. Phenotypic and genetic differences between opaque and translucent colonies of *Vibrio alginolyticus*. *Biofouling.* 2009;25(6):525–531. doi:10.1080/08927010902964578
- [61] Oh EG, Son KT, Yu H, et al. Antimicrobial resistance of *Vibrio parahaemolyticus* and *Vibrio alginolyticus* strains isolated from farmed fish in Korea from 2005 through 2007. *J Food Prot.* 2011;74(3):380–386. doi:10.4315/0362-028X.JFP-10-307